Title

Recursive Parameter Estimation of Thermostatically Controlled Loads via Unscented Kalman Filter

Authors

Burger, Eric M.
Moura, Scott J.

Publication Date

2015-11-30

Recursive Parameter Estimation of Thermostatically Controlled Loads via Unscented Kalman Filter

Eric M. Burger, Scott J. Moura

***Abstract*— For thermostatically controlled loads (TCLs) to perform demand response services in real-time markets, online methods for parameter estimation are needed. As the physical characteristics of a TCL change (e.g. the contents of a refrigerator or the occupancy of a conditioned room), it is necessary to update the parameters of the TCL model. Otherwise, the TCL will be incapable of accurately predicting its potential energy demand, thereby decreasing the reliability of a TCL aggregation to perform demand response. In this paper, we investigate the potential of various unscented Kalman filter (UKF) algorithm variations to recursively identify a TCL model that is nonlinear in the parameters. Experimental results demonstrate the parameter estimation of two residential refrigerators.**

I. Introduction

A. Background and Motivation

Large populations of thermostatically controlled loads (TCLs) hold great potential for performing ancillary services in power systems. The advantages of responsive TCLs over large storage technologies include: (i) they are already well-established technologies; (ii) they are spatially distributed around the power system; (iii) they employ simple and fast local actuation; (iv) they are unimpaired by the outage of individuals in the population; and (v) they - on the aggregate - can produce a quasi-continuous response despite the discrete nature of the individual controls [1][2][3].

Because TCLs are controlled according to a temperature setpoint and deadband range, customers are generally indifferent to precisely when electricity is consumed. The inherent flexibility of TCLs, such as refrigerators and electric water heaters, makes them promising candidates for provisioning power system services. In fact, direct load control (DLC) and demand response (DR) programs are increasingly controlling TCLs, among other electric loads, to improve power grid stability [4][5].

B. Relevant Literature

Past literature on the modelling and control of TCL populations has focused on the development of aggregation methods with centralized control. Malhame and Chong's study [6] is among the first reports to use stochastic analysis to develop an aggregate model of a TCL population. The coupled Fokker-Planck equations, derived in [6], define the aggregate behavior of a homogeneous population. More recently, [7] develops a diffusion-advection partial differential equation (PDE) model and parameter identification scheme for an aggregated population of heterogeneous TCLs. In [8], the authors present a deterministic hybrid PDE-based model for heterogeneous TCL populations, analyze its stability properties, and derive a power reference tracking control law.

In [9], the author uses a linearized Fokker-Planck model to describe the aggregated behavior of a TCL population. Direct control is achieved by broadcasting a single time-varying setpoint temperature offset signal to every agent. Numerical results demonstrate how small perturbations to the setpoint can enable TCLs to perform wind generation following. The work in [10] builds upon [9] by proposing a sliding mode control algorithm for direct control of air conditioning loads. A "state bin" modelling framework is used to describe local states (On/Off) in a discrete temperature-related manner.

In [11], the authors employ a linear time-invariant (LTI) representation of a TCL population. As in [10], a "state bin" modelling framework is used and the aggregate probability mass is allowed to move through these bins. A Markov Chain-based approach is used to predict the evolution of the TCL population. In [3], the authors propose a proportional controller which, at each time step, broadcasts a switching probability, η, to all the TCLs in the population. If $\eta < 0$, all TCLs that are on must switch off with a probability of η and if $\eta > 0$, TCLs that are off switch on with a probability of η.

Recent trends in the field of convex optimization, in particular the introduction of the alternating direction method of multipliers (ADMM), have enabled researchers to pursue distributed methods of load control [1][12][13][14][15]. Therefore, rather than using an aggregation model with centralized control, individual TCLs can coordinate amongst each other to drive the population towards a shared global objective. Because the TCL population is not centrally modeled, a distributed control method is more robust to the loss of agents or to changes in system characteristics. Also, because the individual TCLs are locally optimizing their individual behavior, the central agent requires less information about each TCL's individual characteristics.

However, by controlling TCLs in a distributed manner, it is necessary for every agent in the population to model its own behavior and to predict its energy demand. TCLs with poorly fit models will undermine the ability of the population to accurately perform ancillary services. Given that most TCLs

Corresponding Author: Eric M. Burger, Email: ericburger@berkeley.edu
Affiliation Address: Energy, Control, and Applications Lab (eCAL), 611 Davis Hall, Department of Civil and Environmental Engineering, University of California, Berkeley, Berkeley, CA 94720, USA.

experience regular changes to their physical characteristics (e.g. the contents of a refrigerator, the flow through a water heater, or the occupancy of a conditioned room), a linear time-invariant model is likely to prove inadequate. Also, for TCLs like radiant heaters and air conditioners, it is not possible for the manufacturer to predetermine the physical characteristics of the spaces that will be conditioned. Therefore, to improve the performance of distributed TCL control methods, it is necessary to employ recursive or on-line parameter estimation algorithms to fit and continuously update each TCL's model.

C. Main Contributions

This manuscript contributes to the development of recursive parameter estimation algorithms for TCLs by investigating various unscented Kalman filters for the estimation of a TCL model that is non-linear in the parameters. We present four closely related filter methods (single, joint, dual, and triple) employing both the standard Kalman filter (KF), and unscented Kalman filter (UKF) algorithms. Specifically, we consider: (i) a single filter approach in which one UKF estimates the TCL parameters; (ii) a joint filter approach in which one UKF simultaneously estimates both the parameters and the state; (iii) a dual filter approach in which one UKF estimates the parameters and one KF estimates the state; and (iv) a triple filter approach in which one UKF estimates the parameters, one KF estimates the state, and another KF estimates the model inputs. Finally, we present experimental parameter estimation results using real temperature data from two residential refrigerators.

D. Paper Outline

This paper is organized as follows. Section II discusses the TCL model and Section III overviews the parameter estimation problem. Sections IV and V provide background for the standard Kalman filter (KF) and the unscented Kalman filter (UKF), respectively. Section VI formulates four filter methods for recursive parameter estimation of a TCL. Section VII provides numerical examples of our proposed algorithms. Finally, Section VII summarizes key results.

II. TCL Model

In this paper, a TCL is modeled using the hybrid state discrete time model [1][9][16][17]

$$T^{k+1} = \theta_1 T^k + (1-\theta_1)(T_\infty^k + \theta_2 m^k) + \theta_3 \tag{1a}$$

$$m^{k+1} = \begin{cases} 1 & \text{if } T^k > T_{set} + \frac{\delta}{2} \\ 0 & \text{if } T^k < T_{set} - \frac{\delta}{2} \\ m^k & \text{otherwise} \end{cases} \tag{1b}$$

where state variables $T^k \in \mathbf{R}$ and $m^k \in \{0,1\}$ denote the temperature of the conditioned mass and the discrete state (on or off) of the mechanical system, respectively. Additionally, $k \in \mathbf{Z}$ denotes the integer-valued time step, $T_\infty^k \in \mathbf{R}$ the ambient temperature (°C), $T_{set} \in \mathbf{R}$ the temperature setpoint (°C), and $\delta \in \mathbf{R}$ the temperature deadband width (°C).

In this paper, we will define the time elapsed between each time step as $h = 1/60$ (hours). The parameter θ_1 represents the thermal characteristics of the conditioned mass as defined by $\theta_1 = \exp(-h/RC)$ where C is the thermal capacitance (kWh/°C) and R is the thermal resistance (°C/kW), θ_2 the energy transfer to or from the mass due to the systems operation as defined by $\theta_2 = RP$ where P is the rate of energy transfer (kW), and θ_3 an additive noise process accounting for energy gain or loss not directly modeled. The sign conventions in (1) assume that the TCL is providing a cooling load and that P (and thus θ_2) is negative.

As noted in [9][17], the discrete time model implicitly assumes that all changes in mechanical state occur on the time steps of the simulation. In this paper, we will assume that this behavior reflects the programming of the systems being modeled. In other words, we will assume that the TCLs have a thermostat sampling frequency of $1/h$ Hz or once per minute.

III. Parameter Estimation Background

A fundamental machine learning problem involves the identification of a nonlinear mapping

$$y^k = G(x^k, \theta) \tag{2}$$

where variable $x^k \in \mathbf{R}^X$ is the input, $y^k \in \mathbf{R}^Y$ is the output, and the nonlinear map G is parameterized by $\theta \in \mathbf{R}^\Theta$. Additionally, k denotes the integer-valued time step and X, Y, and Θ are the number of inputs, outputs, and parameters, respectively.

A. Batch Parameter Estimation

Learning can be performed in a batch manner by producing estimates of the parameters $\hat{\theta}$ given a training set of observed inputs and desired outputs, $\{x, y\}$. The goal of a parameter estimation algorithm is to minimize some function of the error between the desired and estimated outputs as given by $e^k = y^k - G(x^k, \hat{\theta})$.

B. Recursive Parameter Estimation

The parameter estimation problem can be expressed in a recursive form using a discrete-time state-space model representation

$$\theta^k = \theta^{k-1} + n^k \tag{3a}$$

$$y^k = G(x^k, \theta^k) + e^k \tag{3b}$$

where θ^k represents the parameter estimates at time step k and $n^k \in \mathbf{R}^\Theta$ corresponds to the parameter update noise (i.e. change in parameter values). The goal of a recursive parameter estimation algorithm is to produce $\hat{\theta}^k$ so as to minimize some function of the error e^k.

IV. Kalman Filter Background

The Kalman filter (KF) is a recursive estimator for linear models such as the discrete-time state-space model

$$x^k = Ax^{k-1} + Bu^k + v^k \tag{4a}$$

$$y^k = Cx^k + Du^k + w^k \tag{4b}$$

where variable $x^k \in \mathbf{R}^X$ is the state of the system, $u^k \in \mathbf{R}^U$ is the known exogenous input, and $y^k \in \mathbf{R}^Y$ is the observed

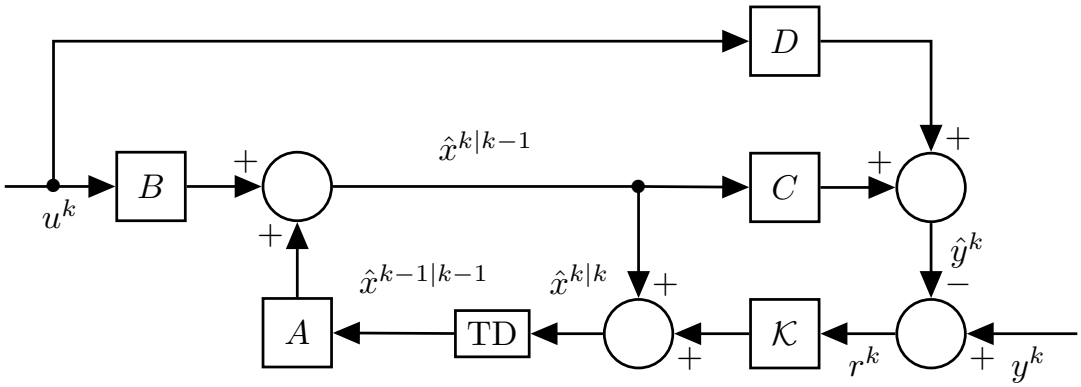

Fig. 1: Kalman Filter Diagram

measurement signal. The state transition model is given by $A \in \mathbf{R}^{X\times X}$ and the control-input model by $B \in \mathbf{R}^{X\times U}$. The process noise $v^k \in \mathbf{R}^X$ has covariance $Q_v \in \mathbf{R}^{X\times X}$, $v^k \sim N(0, Q_v)$. The observation model is given by $C \in \mathbf{R}^{Y\times X}$ and the feedthrough model by $D \in \mathbf{R}^{Y\times U}$. The measurement noise $w^k \in \mathbf{R}^Y$ has covariance $Q_w \in \mathbf{R}^{Y\times Y}$, $w^k \sim N(0, Q_w)$. The variances of v^k and w^k (i.e. diagonal elements of Q_v and Q_w, respectively) must be known in order to implement a Kalman filter.

The Kalman filter (KF) algorithm consists of a prediction step and an update/correction step. The KF will model x^k as a Gaussian random variable (GRV) with estimated mean $\hat{x}^k \in \mathbf{R}^X$ and covariance $Q_x^k \in \mathbf{R}^{X\times X}$. To provide clarity, it is helpful to expand the k notation to distinguish between the state estimates produced before and after the KF correction step. Therefore, at each time step k, the predicted (a priori) state estimate, denoted as $\hat{x}^{k|k-1}$, is the mean estimate of x^k given measurements $y^0, \ldots, y^{k-1}$. The corrected (a posterior) state estimate, $\hat{x}^{k|k}$, is the mean estimate of x^k given measurements $y^0, \ldots, y^k$. To reiterate, throughout this paper, the uncorrected predictions (a priori) are denoted by $k|k-1$ or $k+1|k$ whereas the corrected predictions (a posterior) are denoted by $k|k$, $k-1|k-1$, or $k+1|k+1$.

The KF prediction step is given by

$$\hat{x}^{k|k-1} = A\hat{x}^{k-1|k-1} + Bu^k \tag{5a}$$
$$Q_x^{k|k-1} = AQ_x^{k-1|k-1}A^T + Q_v \tag{5b}$$

and the update/correction step by

$$\hat{y}^k = C\hat{x}^{k|k-1} + Du^k \tag{6a}$$
$$Q_y = CQ_x^{k|k-1}C^T + Q_w \tag{6b}$$

$$\mathcal{K} = Q_x^{k|k-1}C^T Q_y^{-1} \tag{7a}$$
$$r^k = y^k - \hat{y}^k \tag{7b}$$
$$\hat{x}^{k|k} = \hat{x}^{k|k-1} + \mathcal{K}r^k \tag{7c}$$
$$Q_x^{k|k} = Q_x^{k|k-1} - \mathcal{K}Q_y\mathcal{K}^T \tag{7d}$$

Figure 1 illustrates the KF algorithm. The block TD represents a time delay (commonly denoted in controls literature by z^{-1} or $1/z$, the Z-transform of the delay operator). To simplify notation in this paper, we will express the Kalman filter algorithm with the following 3 operator expressions

$$\begin{bmatrix}\hat{x}^{k|k-1}\\ Q_x^{k|k-1}\end{bmatrix} = KF_x\left(\begin{bmatrix}A\\ B\end{bmatrix}, \begin{bmatrix}\hat{x}^{k-1|k-1}\\ Q_x^{k-1|k-1}\end{bmatrix}, u^k, Q_v\right) \tag{8a}$$
$$\begin{bmatrix}\hat{y}^k\\ Q_y^k\end{bmatrix} = KF_y\left(\begin{bmatrix}C\\ D\end{bmatrix}, \begin{bmatrix}\hat{x}^{k|k-1}\\ Q_x^{k|k-1}\end{bmatrix}, u^k, Q_w\right) \tag{8b}$$
$$\begin{bmatrix}\hat{x}^{k|k}\\ Q_x^{k|k}\\ r^k\end{bmatrix} = KF_c\left(\begin{bmatrix}\hat{x}^{k|k-1}\\ Q_x^{k|k-1}\end{bmatrix}, \begin{bmatrix}\hat{y}^k\\ Q_y^k\end{bmatrix}, C, y^k\right) \tag{8c}$$

where (8a) corresponds to (5a-5b), (8b) to (6a-6b), and (8c) to (7a-7d).

V. Unscented Kalman Filter Background

The UKF is an extension to the standard Kalman filter that utilizes a deterministic sampling approach known as the *unscented transform* (UT) to characterize states which undergo a *nonlinear* transformation. The UKF builds on the intuition that it is easier to approximate a probability distribution than to approximate an arbitrary nonlinear transformation [18].

Like the Kalman filter, the UKF includes a prediction step and an update/correction step. However, with the UKF, a state distribution is approximated by a Gaussian random variable (GRV) and specified using a minimal set of sample, or sigma, points around the mean. These sigma points are selected such that they capture the true mean and covariance of the GRV. When propagated through a nonlinear transform, the sigma points accurately capture the a posterior mean and covariance of the estimated state.

In other words, rather than simply passing the previous state estimate $\hat{x}^{k-1}$ through a nonlinear transform to produce a predicted state estimate $\hat{x}^k$, the UKF transforms the set of sigma points. The predicted state estimate $\hat{x}^k$ is then recovered as a weighted mean of the transformed points. With the UT, approximations of Gaussian states are accurate to the third order for any nonlinearities [19]. For non-Gaussian states, approximations are accurate to at least the second-order for any nonlinearities.

In this paper, we employ the UKF algorithm as presented by Wan and van der Merwe [19][20][21] and summarized in the following section. Specifically, see Tables 7.3.1 and 7.3.2 in [20] for the algorithm employed in this work. We direct the reader to [18] for the original presentation of the UT and UKF. A discussion of dual estimation can be found in [19][21].

In the following subsections, we summarize the UKF algorithm as presented by Wan and van der Merwe [20].

A. Sigma Points and Unscented Transform

To detail the UKF algorithm, we begin by describing the generation of sigma points and the execution of the unscented transform (UT). Consider a random variable $s \in \mathbf{R}^L$ with mean $\bar{s} \in \mathbf{R}^L$ and covariance $Q_s \in \mathbf{R}^{L\times L}$ that is propagated through a nonlinear function f such that $z = f(s)$ where $z \in \mathbf{R}^Z$. To calculate the statistics of z, we form a matrix $\mathcal{S} \in \mathbf{R}^{L\times(2L+1)}$ consisting of $2L+1$ sigma points $\mathcal{S}_i$ given by

$$\begin{aligned} \mathcal{S}_0 &= \bar{s} \\ \mathcal{S}_i &= \bar{s} + \left(\sqrt{(L+\lambda)Q_s}\right)_i, \quad i = 1,\ldots,L \\ \mathcal{S}_{i+L} &= \bar{s} - \left(\sqrt{(L+\lambda)Q_s}\right)_i, \quad i = 1,\ldots,L \end{aligned} \tag{9}$$

where $\left(\sqrt{(L+\lambda)Q_s}\right)_i$ is the ith column of the matrix square root of $(L+\lambda)Q_s$ and $\lambda = \alpha^2(L+\kappa) - L$ is a scaling parameter. Constant α determines the spread of the sigma points (usually $10^{-4} \leq \alpha \leq 1$) and constant κ is a secondary scaling parameter (usually $\kappa = 0$ or $3 - L$).

The sigma points are propagated through the nonlinear function

$$\mathcal{Z}_i = f(\mathcal{S}_i) \quad i = 0,\ldots,2L \tag{10}$$

and the mean and covariance of z are approximated as a weighted mean and covariance of the a posterior sigma points

$$\bar{z} \approx \sum_{i=0}^{2L} \mathcal{W}_{m,i}\mathcal{Z}_i \tag{11}$$

$$Q_z \approx \sum_{i=0}^{2L} \mathcal{W}_{c,i}(\mathcal{Z}_i - \bar{z})(\mathcal{Z}_i - \bar{z})^T \tag{12}$$

with weights $\mathcal{W}_m$, corresponding to the a posterior mean of the sigma points, given by

$$\begin{aligned} \mathcal{W}_{m,0} &= \lambda/(L+\lambda) \\ \mathcal{W}_{m,i} &= \lambda/(2(L+\lambda)), \quad i = 1,\ldots,2L \end{aligned} \tag{13}$$

and weights $\mathcal{W}_c$, corresponding to the a posterior covariance of the sigma points, given by

$$\begin{aligned} \mathcal{W}_{c,0} &= \lambda/(L+\lambda) + (1-\alpha+\beta) \\ \mathcal{W}_{c,i} &= \mathcal{W}_{m,i}, \quad i = 1,\ldots,2L \end{aligned} \tag{14}$$

where constant β incorporates prior knowledge of the distribution of s (for Gaussian distributions, $\beta = 2$ is optimal).

To simplify notation, we will denote the generation of sigma points and the execution of the unscented transform ((9)-(12)) with the following operator expressions

$$\mathcal{S} = UT_s(\bar{s}, Q_s) \tag{15a}$$
$$\mathcal{Z}_i = f(\mathcal{S}_i) \quad i = 0,\ldots,2L \tag{15b}$$
$$\bar{z} = UT_m(\mathcal{Z}) \tag{15c}$$
$$Q_z = UT_c(\mathcal{Z}) \tag{15d}$$

where (15a) corresponds to (9), (15c) to (11), and (15d) to (12).

B. Unscented Kalman Filter Algorithm

The unscented Kalman filter (UKF) is a straightforward application of the UT to recursive estimation. To present the UKF algorithm, we will consider the state estimation of a discrete-time nonlinear dynamic system with non-additive noise given by the state-space model

$$x^k = F(x^{k-1}, u^k, v^k) \tag{16a}$$
$$y^k = H(x^k, u^k, w^k) \tag{16b}$$

where variable $x^k \in \mathbf{R}^X$ is the state of the system, $u^k \in \mathbf{R}^U$ is the known exogenous input, and $y^k \in \mathbf{R}^Y$ is the observed measurement signal. Function F is the transition model and the process noise $v^k \in \mathbf{R}^X$ has covariance $Q_v \in \mathbf{R}^{X\times X}$, $v^k \sim N(0, Q_v)$. Function H is the observation model and the measurement noise $w^k \in \mathbf{R}^Y$ has covariance $Q_w \in \mathbf{R}^{Y\times Y}$, $w^k \sim N(0, Q_w)$.

The UKF will model x^k as a GRV with estimated mean $\hat{x}^k$ and covariance Q_x^k. At each time step k, the UKF will generate sigma points for the previous state estimate, $\hat{x}^{k-1|k-1}$. For systems with non-additive noise, the state estimate and covariance is *augmented* with the process and measurement noise, as given by

$$\bar{s}^{k-1} = \begin{bmatrix} \hat{x}^{k-1|k-1} \\ \bar{v}^k \\ \bar{w}^k \end{bmatrix} \tag{17a}$$

$$Q_s^{k-1} = \begin{bmatrix} Q_x^{k-1|k-1} & 0 & 0 \\ 0 & Q_v & 0 \\ 0 & 0 & Q_w \end{bmatrix} \tag{17b}$$

where $\bar{v}^k$ and $\bar{w}^k$ are the mean of the process and measurement noises, respectively. In other words, if Gaussian, $\bar{v}^k \in \{0\}^X$ and $\bar{w}^k \in \{0\}^Y$. The dimensionality of $\bar{s}$ is therefore $L = 2X + Y$.

Next, the UKF will generate the sigma points. Because we are using the augmented state, we will introduce $\mathcal{S}_x$, $\mathcal{S}_v$, and $\mathcal{S}_w$, the sigma points associated with the state estimate, process noise, and measurement noise, respectively.

$$\mathcal{S}^{k-1} = UT_s(\bar{s}^{k-1}, Q_s^{k-1}) \tag{18a}$$
$$\mathcal{S}_{x,j}^{k-1} = \mathcal{S}_j^{k-1} \quad j = 0,\ldots,X-1 \tag{18b}$$
$$\mathcal{S}_{v,j}^{k-1} = \mathcal{S}_j^{k-1} \quad j = X,\ldots,2X-1 \tag{18c}$$
$$\mathcal{S}_{w,j}^{k-1} = \mathcal{S}_j^{k-1} \quad j = 2X,\ldots,2X+Y-1 \tag{18d}$$

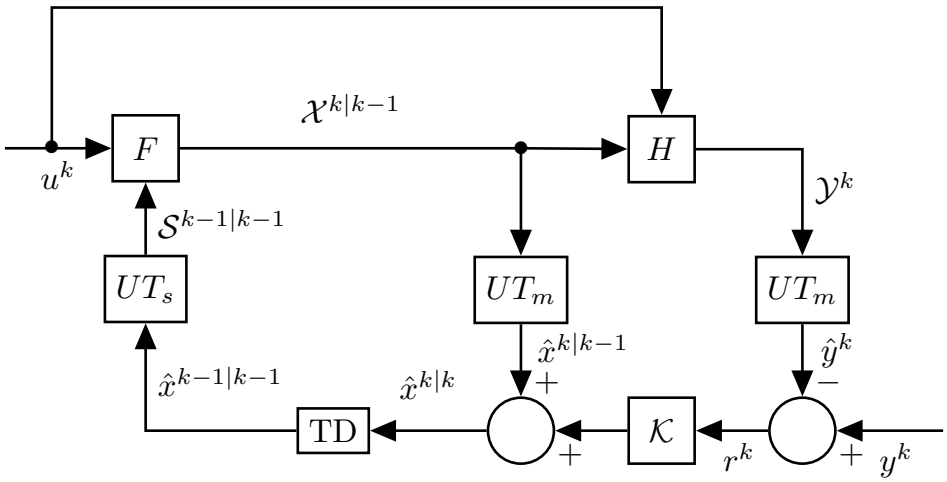

Fig. 2: Additive Unscented Kalman Filter Diagram

where j refers to the rows of the L by $2L+1$ matrix $\mathcal{S}$.

In the prediction step, the UKF will propagate the sigma points through the process model and generate the a priori sigma points $\mathcal{X}_i^{k|k-1}$, state estimate $\hat{x}^{k|k-1}$, and covariance $Q_x^{k|k-1}$ as follows,

$$\mathcal{X}_i^{k|k-1} = F(\mathcal{S}_{x,i}^{k-1}, u^k, \mathcal{S}_{v,i}^{k-1}) \quad i = 0, \ldots, 2L \tag{19a}$$
$$\hat{x}^{k|k-1} = UT_m(\mathcal{X}^{k|k-1}) \tag{19b}$$
$$Q_x^{k|k-1} = UT_c(\mathcal{X}^{k|k-1}) \tag{19c}$$

In the correction step, the UKF will propagate the a priori sigma points through the measurement model to generate the measurement sigma points $\mathcal{Y}_i^k$, estimate $\hat{y}^k$, and covariance Q_y as follows,

$$\mathcal{Y}_i^k = H(\mathcal{X}_i^{k|k-1}, u^k, \mathcal{S}_{w,i}^{k-1}) \quad i = 0, \ldots, 2L \tag{20a}$$
$$\hat{y}^k = UT_m(\mathcal{Y}^k) \tag{20b}$$
$$Q_y = UT_c(\mathcal{Y}^k) \tag{20c}$$

These are used to calculate the cross-covariance Q_{xy}, the Kalman gain $\mathcal{K}$, and the observation error r^k. Finally, the state estimate and covariance are corrected, producing the a posterior estimate $\hat{x}^{k|k}$ and covariance $Q_x^{k|k}$.

$$Q_{xy} = \sum_{i=0}^{2L} \mathcal{W}_{c,i}(\mathcal{X}_i^{k|k-1} - \hat{x}^{k|k-1})(\mathcal{Y}_i^k - \hat{y}^k)^T \tag{21a}$$
$$\mathcal{K} = Q_{xy}Q_y^{-1} \tag{21b}$$
$$r^k = y^k - \hat{y}^k \tag{21c}$$
$$\hat{x}^{k|k} = \hat{x}^{k|k-1} + \mathcal{K}r^k \tag{21d}$$
$$Q_x^{k|k} = Q_x^{k|k-1} - \mathcal{K}Q_y\mathcal{K}^T \tag{21e}$$

where $r^k \in \mathbf{R}$ is the error between the measurement y^k and the estimate $\hat{y}^k$ at time step k.

To simplify notation in this paper, we will express the non-additive unscented Kalman filter algorithm with augmented state using the following 4 operator expressions

$$\begin{bmatrix} \mathcal{S}_x^{k-1} \\ \mathcal{S}_v^{k-1} \\ \mathcal{S}_w^{k-1} \end{bmatrix} = UKF_s\left(\begin{bmatrix} \hat{x}^{k-1|k-1} \\ Q_x^{k-1|k-1} \end{bmatrix}, \begin{bmatrix} \bar{v}^k \\ Q_v \end{bmatrix}, \begin{bmatrix} \bar{w}^k \\ Q_w \end{bmatrix}\right) \tag{22a}$$
$$\begin{bmatrix} \hat{x}^{k|k-1} \\ Q_x^{k|k-1} \\ \mathcal{X}^{k|k-1} \end{bmatrix} = UKF_x\left(F, \mathcal{S}_x^{k-1}, u^k, \mathcal{S}_v^{k-1}\right) \tag{22b}$$
$$\begin{bmatrix} \hat{y}^k \\ Q_y^k \\ \mathcal{Y}^k \end{bmatrix} = UKF_y(H, \mathcal{X}^{k|k-1}, u^k, \mathcal{S}_w^{k-1}) \tag{22c}$$
$$\begin{bmatrix} \hat{x}^{k|k} \\ Q_x^{k|k} \\ r^k \end{bmatrix} = UKF_c\left(\begin{bmatrix} \hat{x}^{k|k-1} \\ Q_x^{k|k-1} \\ \mathcal{X}^{k|k-1} \end{bmatrix}, \begin{bmatrix} \hat{y}^k \\ Q_y^k \\ \mathcal{Y}^k \end{bmatrix}, y^k\right) \tag{22d}$$

where (22a) corresponds to (17-18), (22b) to (19), (22c) to (20), and (22d) to (21).

C. Additive Unscented Kalman Filter

Consider the discrete-time nonlinear dynamic system with additive noise,

$$x^k = F(x^{k-1}, u^k) + v^k \tag{23a}$$
$$y^k = H(x^k, u^k) + w^k \tag{23b}$$

In this (very common) case, the UKF algorithm can be simplified. Specifically, $\bar{s}^{k-1} = \hat{x}^{k-1|k-1}$, $Q_s^{k-1} = Q_x^{k-1|k-1}$, and there are no sigma points for the process and measurement noise. This reduces the computational complexity of each iteration of the UKF from $O((2X+Y)^3)$ to $O(X^3)$ where X is the dimensionality of the state space and Y the dimensionality of the observation space. The complete additive UKF algorithm for model (23) is therefore,

$$\mathcal{S}_x^{k-1} = UT_s(\hat{x}^{k-1|k-1}, Q_x^{k-1|k-1}) \tag{24a}$$
$$\mathcal{X}_i^{k|k-1} = F(\mathcal{S}_{x,i}^{k-1}, u^k) \quad i = 0, \ldots, 2X \tag{24b}$$
$$\hat{x}^{k|k-1} = UT_m(\mathcal{X}^{k|k-1}) \tag{24c}$$

$$Q_x^{k|k-1} = UT_c(\mathcal{X}^{k|k-1}) + Q_v \tag{24d}$$
$$\mathcal{Y}_i^k = H(\mathcal{X}_i^{k|k-1}, u^k) \quad i = 0, \ldots, 2X \tag{24e}$$
$$\hat{y}^k = UT_m(\mathcal{Y}^k) \tag{24f}$$
$$Q_y = UT_c(\mathcal{Y}^k) + Q_w \tag{24g}$$
$$Q_{xy} = \sum_{i=0}^{2L} \mathcal{W}_{c,i}(\mathcal{X}_i^{k|k-1} - \hat{x}^{k|k-1})(\mathcal{Y}_i^k - \hat{y}^k)^T \tag{24h}$$
$$\mathcal{K} = Q_{xy}Q_y^{-1} \tag{24i}$$
$$r^k = y^k - \hat{y}^k \tag{24j}$$
$$\hat{x}^{k|k} = \hat{x}^{k|k-1} + \mathcal{K}r^k \tag{24k}$$
$$Q_x^{k|k} = Q_x^{k|k-1} - \mathcal{K}Q_y\mathcal{K}^T \tag{24l}$$

Figure 2 illustrates the additive UKF algorithm. The block TD represents a time delay (commonly denoted in controls literature by z^{-1} or $1/z$, the Z-transform of the delay operator). To simplify notation in this paper, we will express the additive unscented Kalman filter algorithm using the following 4 operator expressions

$$\left[\mathcal{S}_x^{k-1}\right] = UKF_s^+\left(\begin{bmatrix}\hat{x}^{k-1|k-1}\\ Q_x^{k-1|k-1}\end{bmatrix}\right) \tag{25a}$$
$$\begin{bmatrix}\hat{x}^{k|k-1}\\ Q_x^{k|k-1}\\ \mathcal{X}^{k|k-1}\end{bmatrix} = UKF_x^+\left(F, \mathcal{S}_x^{k-1}, u^k, Q_v\right) \tag{25b}$$
$$\begin{bmatrix}\hat{y}^k\\ Q_y^k\\ \mathcal{Y}^k\end{bmatrix} = UKF_y^+(H, \mathcal{X}^{k|k-1}, u^k, Q_w) \tag{25c}$$
$$\begin{bmatrix}\hat{x}^{k|k}\\ Q_x^{k|k}\\ r^k\end{bmatrix} = UKF_c^+\left(\begin{bmatrix}\hat{x}^{k|k-1}\\ Q_x^{k|k-1}\\ \mathcal{X}^{k|k-1}\end{bmatrix}, \begin{bmatrix}\hat{y}^k\\ Q_y^k\\ \mathcal{Y}^k\end{bmatrix}, y^k\right) \tag{25d}$$

where (25a) corresponds to (24a), (25b) to (24b-24d), (25c) to (24e-24g), and (25d) to (24h-24l).

VI. Recursive TCL Parameter Estimation

In this section, we will present 4 closely related approaches for parameter estimation of a thermostatically controlled load (TCL) using the Kalman filter (KF) algorithm in (8) and unscented Kalman filter (UKF) algorithm in (25). In this paper, we will consider: (i) a single filter approach in which one UKF is used to estimate the parameters θ^k; (ii) a joint filter approach in which one UKF simultaneously estimates both θ^k and T^k; (iii) a dual filter approach in which one UKF estimates the parameters θ^k and one KF estimates the state T^k; and (iv) a triple filter approach in which we use one UKF to estimate θ^k, one KF to estimate T^k, and another KF to estimate the inputs, T_∞^k and m^k.

In each case, we define the function G according to the TCL model (1)

$$\begin{aligned} T^{k+1} &= \theta_1^k T^k + \begin{bmatrix}1-\theta_1^k & 1-\theta_1^k\theta_2^k & \theta_3^k\end{bmatrix}\begin{bmatrix}T_\infty^k\\ m^k\\ 1\end{bmatrix} \\ &= G(T^k, T_\infty^k, m^k, \theta^k) \end{aligned} \tag{26}$$

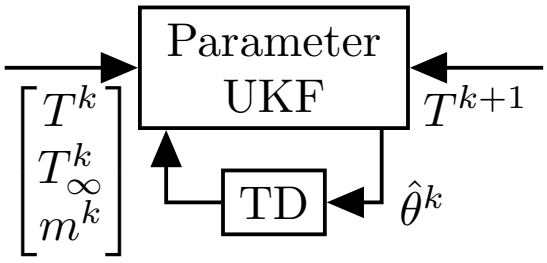

Fig. 3: Single Filter Method Diagram

A. Single Filter Parameter Estimation

Using the function G given in (26), the TCL recursive parameter estimation problem can be expressed with the state-space model

$$\theta^k = \theta^{k-1} + n^k \tag{27a}$$
$$y^k = G(T^k, T_\infty^k, m^k, \theta^k) + v^k + w^k \tag{27b}$$

where (27b) combines (26) with observation model $y^k = T^{k+1} + w^k$.

Figure 3 illustrates the single filter method. The block TD represents a time delay (commonly denoted $1/z$, the Z-transform of the delay operator). By employing the additive UKF algorithm in (25) with the T^{k+1} observation as y^k, we can produce $\hat{\theta}^k$, an estimate of the model parameters at time step k. Note that in the single filter case, θ corresponds to x, the variable being estimated, and G to H, the observation model. Additionally, the transition model F is given by $F(x^{k-1}, u^k) = x^{k-1}$ and T^k, T_∞^k, and m^k are effectively u^k, control and feed-through inputs at time step k.

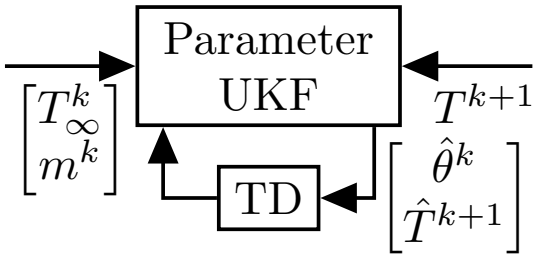

Fig. 4: Joint Filter Method Diagram

B. Joint Filter State and Parameter Estimation

For system identification, it is often necessary to simultaneous perform state and parameter estimation from noisy observations [19]. There are two basic approaches, joint and dual estimation. In the joint estimation method, state and parameter estimation can be performed simultaneously with a single filter by estimating the state-space model

$$\begin{bmatrix}\theta^k\\ T^{k+1}\end{bmatrix} = \begin{bmatrix}\theta^{k-1}\\ G(T^k, T_\infty^k, m^k, \theta^{k-1})\end{bmatrix} + \begin{bmatrix}n^k\\ v^k\end{bmatrix} \tag{28a}$$
$$y^k = T^{k+1} + w^k \tag{28b}$$

Figure 4 illustrates the joint filter method where the block TD represents a time delay. Just as in the single filter

method, we employ the additive UKF algorithm in (25) with the T^{k+1} observation as y^k to recursively estimate the model. However, in the joint filter method, we produce estimates of both the state and the parameters ($\hat{T}^{k+1}$ and $\hat{\theta}^k$, respectively).

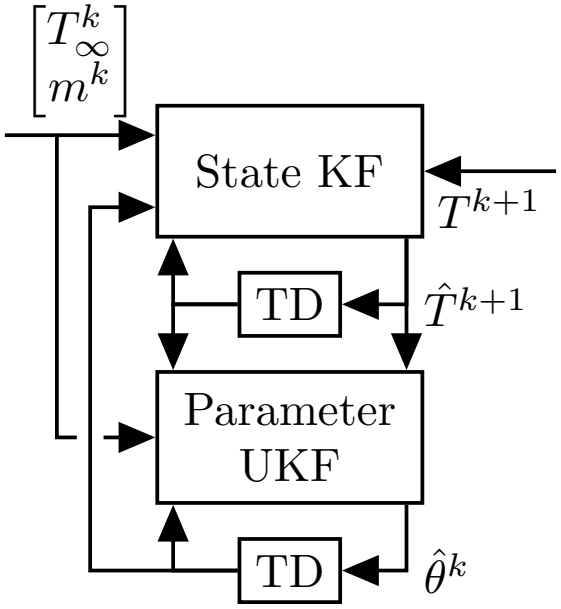

Fig. 5: Dual Filter Method Diagram

C. Dual Filter State and Parameter Estimation

In the dual estimation method, a separate state-space representation is used for the states and parameters. For a TCL, the state model is given by

$$T^{k+1} = G(T^k, T_\infty^k, m^k, \theta^k) + v^k \tag{29a}$$
$$y^k = T^{k+1} + w^k \tag{29b}$$

and the parameter model by (27).

Figure 5 illustrates the dual filter method where the block TD represents a time delay. Because the function G is linear in the states, we can estimate the state model (29) using the KF algorithm in (8) with the T^{k+1} observation as y^k to produce $\hat{T}^{k+1}$. Again, the parameter model (27) is estimated using the additive UKF algorithm in (25). We tie the two filters together by using the estimated state of one filter as the control input and/or observation in another filter. Specifically, for the state filter, we use the previous parameter estimate $\hat{\theta}^{k-1}$ in the transition model. For the parameter filter, we use the previous estimate $\hat{T}^k$ as input in the observation model and the current estimate $\hat{T}^{k+1}$ as the observation y^k (rather than the T^k and T^{k+1} observations, respectively).

D. Triple Filter Input, State, and Parameter Estimation

Lastly, we consider an estimation approach in which separate filters are used to estimate the inputs, states, and parameters. For simplicity, we will refer to this as the triple filter approach. The input model is given by

$$\begin{bmatrix} T_\infty^k \\ m^k \end{bmatrix} = \begin{bmatrix} T_\infty^{k-1} \\ m^{k-1} \end{bmatrix} + \begin{bmatrix} p_1^k \\ p_2^k \end{bmatrix} \tag{30a}$$
$$y^k = \begin{bmatrix} G(T^k, T_\infty^k, m^k, \theta^{k-1}) \\ T_\infty^k \\ m^k \end{bmatrix} + \begin{bmatrix} v^k + w^k \\ q_1^k \\ q_2^k \end{bmatrix} \tag{30b}$$

where $p \in \mathbf{R}^2$ and $q \in \mathbf{R}^2$ are process and measurement noises, respectively, associated with the inputs T_∞ and m. Again, the state model is given by (29) and the parameter model by (27).

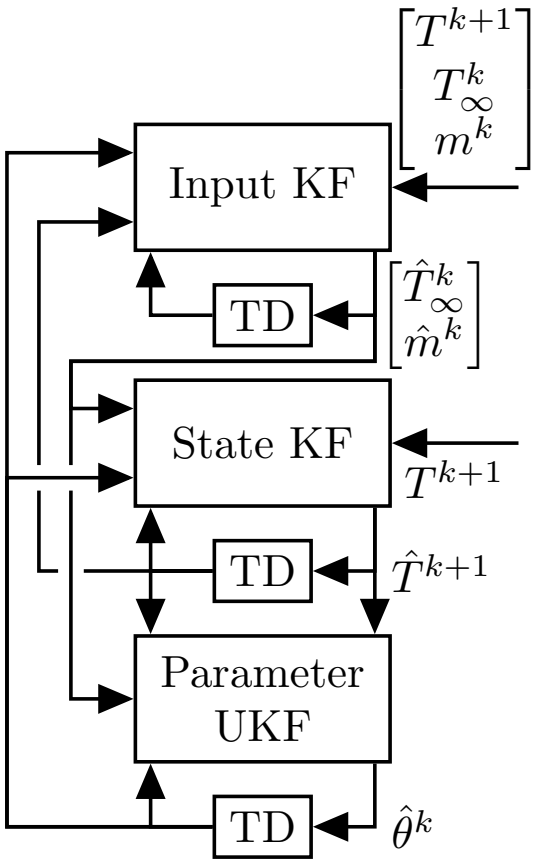

Fig. 6: Triple Filter Method Diagram

Figure 6 illustrates the triple filter method where the block TD represents a time delay. The input model (30) is estimated using the KF algorithm in (8) with the T^{k+1}, T_∞^k, and m^k observations as y^k to produce $\hat{T}_\infty^k$ and $\hat{m}^k$. To tie the three models together, the input estimates $\hat{T}_\infty^k$ and $\hat{m}^k$ are used in the transition model of the state filter and the observation model of the parameter filter. The previous parameter estimate $\hat{\theta}^{k-1}$ is used in the observation model of the input filter and the transition model of the state filter. Lastly, the state estimate $\hat{T}^k$ is used in the observation model of the input and parameter filters and $\hat{T}^{k+1}$ serves as the observation y^k in the parameter filter.

VII. TCL Estimation Experimental Results

In this section, we present parameter estimation results for TCL_1, a 500W residential refrigerator, and TCL_2, a

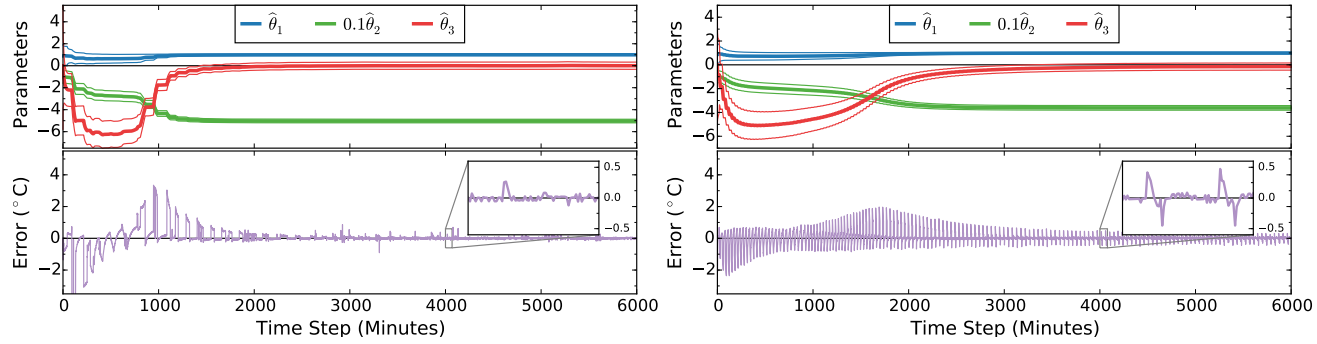

(a) TCL_1 (b) TCL_2

Fig. 7: Single Filter Parameter Estimation

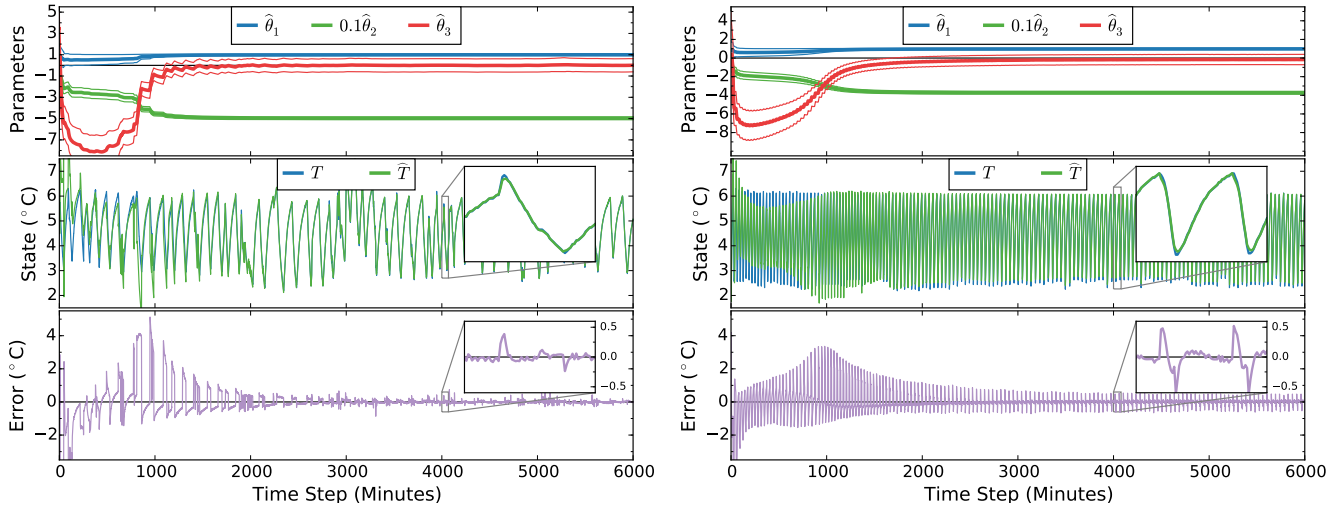

(a) TCL_1 (b) TCL_2

Fig. 8: Joint Filter Parameter Estimation

100W mini-fridge. Each TCL is instrumented with two DS18B20 digital temperature sensors to measure the ambient temperature T_∞ and internal refrigerator temperature T. The sensors have a $-55°\text{C}$ to $+125°\text{C}$ temperature range and a $\pm 0.5°\text{C}$ accuracy from $-10°\text{C}$ to $+85°\text{C}$. A current sensor is used to measure the state (on or off) of the compressor, m. Measurements were taken at 1 minute intervals for a period of 7 days. In this study, the temperature of the freezer is neither measured nor modeled.

TCL_1 is observed under typical operating conditions for a residential refrigerator. Therefore, the door is opened randomly and the contents of the refrigerator change regularly. By contrast, TCL_2 is empty except for 18 liters of water, which compose the thermal mass being conditioned by the unit. The door of TCL_2 remains closed for the duration of the study.

For both TCLs, we have implemented four parameter estimation methods using the standard and unscented Kalman filters: single filter, joint filter, dual filter, and triple filter. The final parameter estimates $\hat{\theta}^f$ are presented in Table I. Normally, for system identification, we would seek to measure the performance of each algorithm by first learning the parameters using a training dataset and then testing the parameters using a separate validation dataset. However, an advantage of recursive parameter estimation is that we can continuously improve the parameter estimates and potentially adapt to changes in the mechanical system. Therefore, for the single, dual, joint, and triple filter methods, we represent the performance as the root mean squared error (RMSE) over the last 300 time steps (i.e 5 hours). We will denote this moving window RMSE as RMSE300. To measure the parameter estimation error, we employ the residual error r^k of the parameter filter for each of the four methods.

Figure 7 presents the parameter estimation results using the single filter method. The top subplots show the parameter estimates $\hat{\theta}^k$ produced by the parameter filter at each time step k. For each parameter, the center line is the mean or expected value of the estimate and the top and bottom lines illustrate the variance relative to the mean. Eventually all parameter estimates converge and the variances decrease. The bottom subplots depict the residual error r^k. As shown, the parameter estimation for TCL_1 converges in about 1500

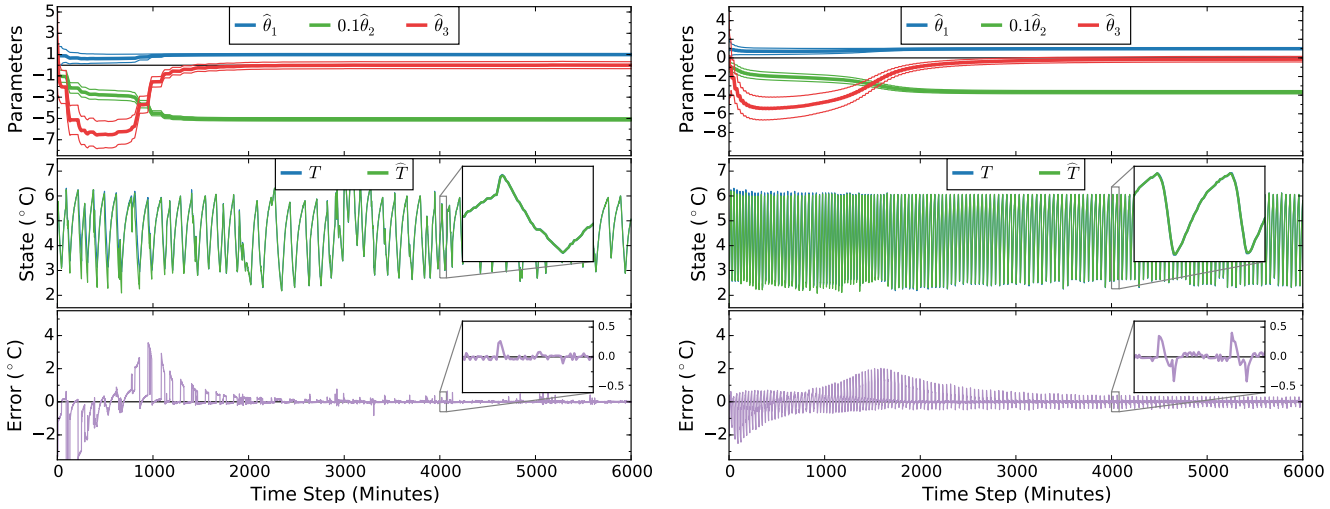

(a) TCL_1 (b) TCL_2

Fig. 9: Dual Filter Parameter Estimation

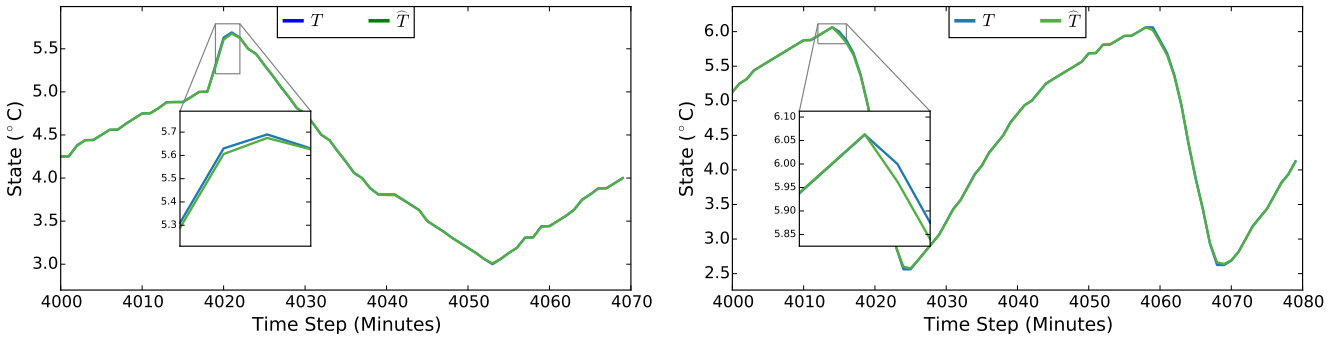

(a) TCL_1 (b) TCL_2

Fig. 10: Dual Filter Temperature State Estimate

	TCL_1			TCL_2		
	$\hat{\theta}_1^f$	$\hat{\theta}_2^f$	$\hat{\theta}_3^f$	$\hat{\theta}_1^f$	$\hat{\theta}_2^f$	$\hat{\theta}_3^f$
Single	0.998	-50.329	0.004	0.987	-36.193	-0.141
Joint	0.997	-49.762	0.005	0.985	-37.277	-0.159
Dual	0.998	-50.872	0.004	0.988	-36.822	-0.133
Triple	0.997	-52.268	0.005	0.986	-37.141	-0.153

TABLE I: Final Parameter Estimates for TCL_1 and TCL_2

time steps while TCL_2 converges in about 3000 time steps.

Figure 8 presents the parameter estimation results using the joint filter method and Fig. 9 for the dual filter method. Again, the top subplots show the parameter estimates $\hat{\theta}^k$. The bottom subplots depict the residual error r^k. The state estimates $\hat{T}^k$ are presented in the center subplots. Both TCLs exhibit similar convergence characteristics compared to the single filter method. Upon convergence, the difference between the measured temperature T and estimated temperature $\hat{T}$ becomes negligible. A sample of the temperature estimates produced by the dual filter are shown in Fig. 10.

As shown in Table I, the differences in the final TCL_1 and TCL_2 parameter estimates for the single, joint, and dual filters are small enough to be considered negligible. Thus, with respect to parameter estimation, the joint and dual filters show little to no advantage over the single filter method. In other words, filtering the temperature measurement T does not appear to significantly improve the performance of our parameter estimation algorithm. Considering that we are estimating the parameters of two residential-sized refrigerators, this is not a surprising outcome. For a larger or noisier TCL, the joint and dual filters may yield a greater advantage, but for the TCLs used in this study, the estimation of T is simply unnecessary.

Figure 11 presents the parameter estimation results using the triple filter method. In addition to the parameter estimate $\hat{\theta}^k$, state estimate $\hat{T}^k$, and parameter filter residual error r^k, the figure displays the compressor state estimates $\hat{m}^k$. The input filters also produce ambient temperature estimates $\hat{T}_\infty^k$. However, due to the negligible difference between the ambient temperature observations and estimates, we have excluded the results from this manuscript.

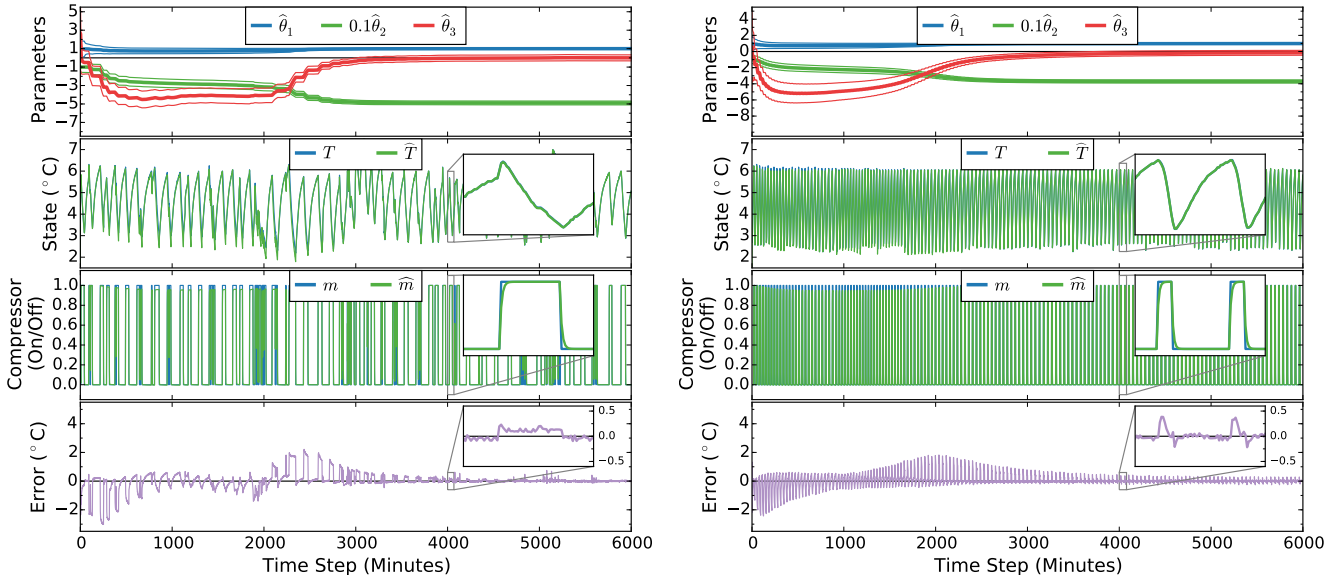

(a) TCL_1 (b) TCL_2

Fig. 11: Triple Filter Parameter Estimation

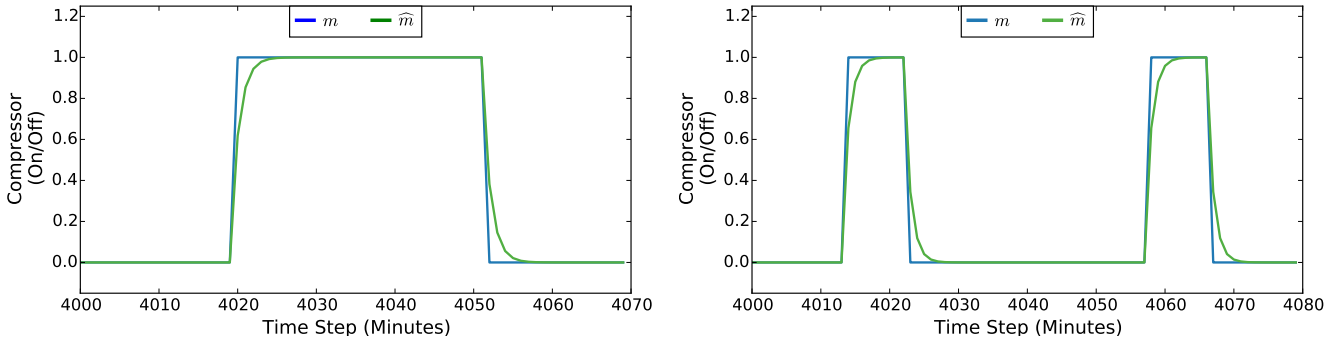

(a) TCL_1 (b) TCL_2

Fig. 12: Triple Filter Compressor State Estimate

A sample of the compressor state estimates are plotted in Fig. 12. As shown in Fig. 12, the estimated compressor states $\hat{m}^k$ resemble a first-order system response rather than the discrete on/off state m^k given by the TCL model (1). One could argue that $\hat{m}^k$ better represents the thermodynamics of a TCL like the refrigerators used in this study. Specifically, while the compressor may instantaneously turn on or off (providing a step input), it takes some amount of time for the refrigeration cycle to start or stop removing heat (resulting in a first-order response). We could elect to model the refrigeration cycle as a first-order linear time-invariant system and to estimate the system parameters, however using the triple filter method to estimate m^k is a simple way to achieve a comparable result.

The moving window root mean square error (RMSE) results for each filter method are presented in Figure 13. As stated previously, the RMSE300 at each time step is a measure of the RMSE over the last 300 time steps (i.e 5 hours). In this way, the RMSE300 is a function of the parameter filter's residual error r^k but provides a clearer means of comparing the performance of each filter method. As shown in Figure 13, the triple filter is the slowest to converge but performs slightly better than the other methods. The single and joint filter performances are comparable in TCL_1 whereas the joint method has the worst performance for TCL_2. Overall, each filter method succeeds in performing parameter estimation and converges to comparable values. After convergence, the differences in the RMSE300 values are small enough to be considered negligible, suggesting that the refrigerators studied in this paper are relatively low noise systems. The same results are not to be expected of larger or noisier TCLs. Nonetheless, this manuscript presents a compiled collection of filtering methods for online learning of TCLs.

Utilizing a recursive system identification technique provides the added benefit of allowing the parameter estimates to adapt to changes in the system. To illustrate this point, we removed the 18 liters of water from TCL_2 at roughly time

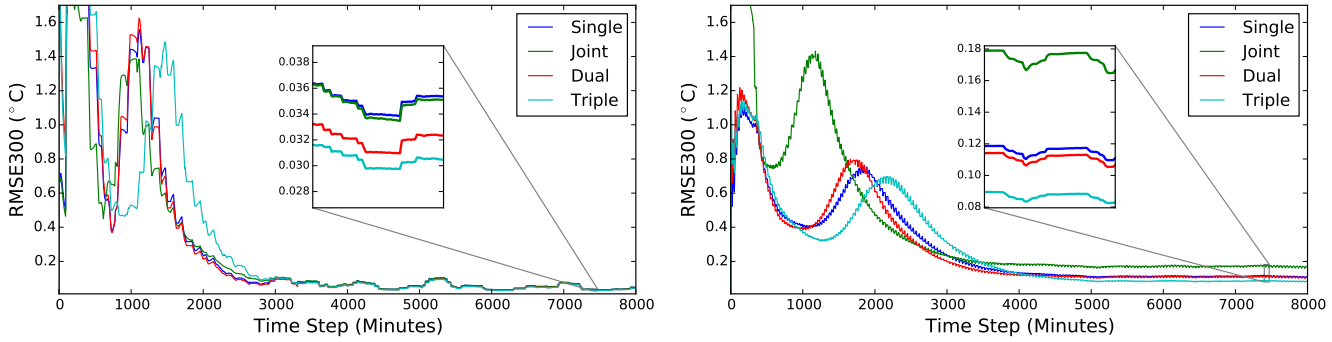

(a) TCL_1 (b) TCL_2

Fig. 13: Parameter Estimation Moving Window RMSE

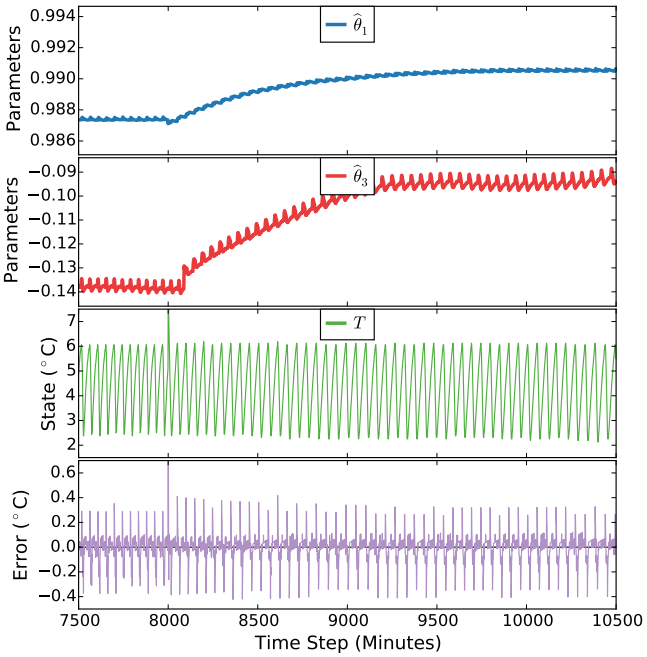

Fig. 14: TCL_2 Adaptive Parameter Estimation

step $k = 8000$, thereby reducing the thermal capacitance of the system. Figure 14 illustrates how the single UKF method responded to this change by increasing both $\hat{\theta}_1$ and $\hat{\theta}_3$. According to the TCL model (1), we expect that decreasing the capacitance in the TCL increases $\hat{\theta}_1$, which represents the thermal characteristics of the conditioned mass ($\theta_1 = \exp(-h/RC)$). As stated previously, $\hat{\theta}_3$ represents a noise process accounting for energy gain or loss that is not directly modeled. The parameter estimates converge to new values within about 1000 time steps, thus demonstrating the real-time estimation feature of the algorithms studied here.

VIII. Conclusions

This paper examines online parameter estimation of thermostatically controlled loads (TCLs). The specific context is modeling and distributed control of aggregated loads for power system services, such as load following and frequency regulation. In this paper, we briefly discuss the Kalman filter (KF) and unscented Kalman filter (UKF) algorithms. Next, we present four filter methods (single, joint, dual, and triple) for recursively estimating the parameters of a discrete-time thermostatically controlled load (TCL) model. Finally, we present experimental results using real temperature data from a 500W and a 100W residential refrigerator. For each of the four filter methods, the algorithm successfully converges to comparable parameter estimates and adapts to changing TCL characteristics.

References

[1] E. M. Burger and S. J. Moura, "Generation Following with Thermostatically Controlled Loads via Alternating Direction Method of Multipliers Sharing Algorithm," October 2015, In Review. [Online]. Available: http://escholarship.org/uc/item/2m5333xx

[2] D. S. Callaway, I. Hiskens *et al.*, "Achieving controllability of electric loads," *Proceedings of the IEEE*, vol. 99, no. 1, pp. 184–199, 2011.

[3] J. L. Mathieu, S. Koch, and D. S. Callaway, "State estimation and control of electric loads to manage real-time energy imbalance," *Power Systems, IEEE Transactions on*, vol. 28, no. 1, pp. 430–440, 2013.

[4] J. Eto, J. Nelson-Hoffman, C. Torres, S. Hirth, B. Yinger, J. Kueck, B. Kirby, C. Bernier, R. Wright, A. Barat *et al.*, "Demand response spinning reserve demonstration. lawrence berkeley national laboratory, berkeley, ca. prepared for energy systems integration," *Public Interest Energy Research Program, California Energy Commission*, 2007.

[5] J. L. Mathieu and D. S. Callaway, "State estimation and control of heterogeneous thermostatically controlled loads for load following," in *System Science (HICSS), 2012 45th Hawaii International Conference on*. IEEE, 2012, pp. 2002–2011.

[6] R. Malhame and C.-Y. Chong, "Electric load model synthesis by diffusion approximation of a high-order hybrid-state stochastic system," *Automatic Control, IEEE Transactions on*, vol. 30, no. 9, pp. 854–860, 1985.

[7] S. Moura, V. Ruiz, and J. Bendsten, "Modeling heterogeneous populations of thermostatically controlled loads using diffusion-advection pdes," in *ASME 2013 Dynamic Systems and Control Conference*. American Society of Mechanical Engineers, 2013, pp. V002T23A001–V002T23A001.

[8] A. Ghaffari, S. Moura, and M. Krstic, "Pde-based modeling, control, and stability analysis of heterogeneous thermostatically controlled load populations," *Journal of Dynamic Systems, Measurement, and Control*, 2015.

[9] D. S. Callaway, "Tapping the energy storage potential in electric loads to deliver load following and regulation, with application to wind energy," *Energy Conversion and Management*, vol. 50, no. 5, pp. 1389–1400, May 2009.

[10] S. Bashash and H. K. Fathy, "Modeling and control insights into demand-side energy management through setpoint control of thermostatic loads," in *American Control Conference (ACC), 2011*. IEEE, 2011, pp. 4546–4553.

[11] S. Koch, J. L. Mathieu, and D. S. Callaway, "Modeling and control of aggregated heterogeneous thermostatically controlled loads for ancillary services," in *Proc. PSCC*, 2011, pp. 1–7.

[12] S. Boyd, N. Parikh, E. Chu, B. Peleato, and J. Eckstein, "Distributed optimization and statistical learning via the alternating direction method of multipliers," *Foundations and Trends in Machine Learning*, vol. 3, no. 1, pp. 1–122, January 2011.

[13] A. Mercurio, A. Di Giorgio, and F. Purificato, "Optimal fully electric vehicle load balancing with an admm algorithm in smartgrids," in *Control & Automation (MED), 2013 21st Mediterranean Conference on*. IEEE, 2013, pp. 119–124.

[14] H. Xing, Y. Mou, Z. Lin, and M. Fu, "Fast distributed power regulation method via networked thermostatically controlled loads," vol. 19, Cape Town, South Africa, 2014, pp. 5439 – 5444.

[15] M. Liu and Y. Shi, "Distributed model predictive control of thermostatically controlled appliances for providing balancing service," in *2014 IEEE 53rd Annual Conference on Decision and Control (CDC)*, Dec 2014, pp. 4850–4855.

[16] S. Ihara and F. C. Schweppe, "Physically based modeling of cold load pickup," *IEEE Transactions on Power Apparatus and Systems*, vol. 100, no. 9, pp. 4142–4250, 1981.

[17] R. E. Mortensen and K. P. Haggerty, "A stochastic computer model for heating and cooling loads." *IEEE Transactions on Power Systems*, vol. 3, no. 3, pp. 1213–1219, Aug 1998.

[18] S. J. Julier and J. K. Uhlmann, "New extension of the kalman filter to nonlinear systems," in *AeroSense'97*. International Society for Optics and Photonics, 1997, pp. 182–193.

[19] E. A. Wan, R. Van Der Merwe, and A. T. Nelson, "Dual Estimation and the Unscented Transformation," in *NIPS*. Citeseer, 1999, pp. 666–672.

[20] E. A. Wan and R. V. D. Merwe, "The Unscented Kalman Filter," in *Kalman Filtering and Neural Networks*. Wiley, 2001, pp. 221–280.

[21] E. Wan, R. Van Der Merwe *et al.*, "The unscented Kalman filter for nonlinear estimation," in *Adaptive Systems for Signal Processing, Communications, and Control Symposium 2000. AS-SPCC. The IEEE 2000*. IEEE, 2000, pp. 153–158.